Salicylic acid perturbs small RNA-gibberellin regulatory network in immune response of potato to *Potato virus Y* infection and renders plants tolerant to the pathogen

Maja Križnik[1,2], Marko Petek[1], David Dobnik[1], Živa Ramšak[1], Špela Baebler[1], Stephan Pollmann[3], Jan Kreuze[4], Jana Žel[1], Kristina Gruden[1]

[1]Department of Biotechnology and Systems Biology, National Institute of Biology, Ljubljana 1000, Slovenia

[2]Jožef Stefan International Postgraduate School, Ljubljana 1000, Slovenia

[3]Centro de Biotecnología y Genómica de Plantas, Universidad Politécnica de Madrid (UPM) - Instituto Nacional de Investigación y Tecnología Agraria y Alimentaria (INIA), Campus de Montegancedo UPM, Madrid 28223, Spain.

[4]Global Program of Integrated Crop and Systems Research, International Potato Center (CIP), Lima 12, Peru

Abstract

Potato virus Y is the most economically important potato viral pathogen. We aimed at unraveling the roles of small RNAs (sRNAs) in the complex immune signaling network controlling the establishment of tolerant response of potato cv. Désirée to the virus. We constructed a sRNA regulatory network connecting sRNAs and their targets to link sRNA level responses to physiological processes. We discovered an interesting novel sRNAs-gibberellin regulatory circuit being activated as early as 3 days post inoculation, before viral multiplication can be detected. Increased levels of miR167 and phasiRNA931 were reflected in decreased levels of transcripts involved in gibberellin biosynthesis. Moreover, decreased concentration of gibberellin confirmed this regulation. The functional relation between lower activity of gibberellin signaling and reduced disease severity was previously confirmed in Arabidopsis-virus interaction using knockout mutants. We additionally showed that this regulation is salicylic acid dependent as the response of sRNA network was attenuated in salicylic acid-depleted transgenic counterpart NahG-Désirée expressing severe disease

symptoms. Besides downregulation of gibberellin signaling, regulation of several other parts of sRNA network in tolerant Désirée revealed similarities to responses observed in mutualistic symbiotic interactions. The intertwining of different regulatory networks revealed shows how developmental signaling, symptomology and stress signaling are balanced.

Introduction

Potato (*Solanum tuberosum* L.) is the world's most important non-grain staple crop. Viruses pose a serious threat to potato production, not only because of the effects caused by the primary infection, but also because potato is propagated vegetatively so that viruses are transmitted through the tubers and accumulate over time (Solomon-Blackburn and Barker, 2001). The most devastating potato virus is *Potato virus Y* (PVY) (Karasev and Gray, 2013). PVY is a member of the Potyviridae family and comprises of many diverse strains. Worldwide, the most harmful strain is PVY^{NTN} which has been responsible for huge decreases in quality and quantity of potato tuber production (Scholthof et al., 2011). One of the most widely grown potato cultivars is cv. Désirée, which is tolerant to PVY^{NTN}, meaning that the virus replicates and spreads systemically, however, symptoms of the disease are reduced or not visible at all (Ravnikar, 2013; Baebler et al., 2011). Tolerance may have an advantage over resistance for crop protection because it does not actively prevent virus infection and/or replication, therefore there is little evolutionary pressure for PVY to mutate and to evolve into more aggressive strains (Bosch et al., 2006). Hence, the tolerant phenotype is likely to be more durable than resistance (Wilson, 2014). Until now, studies on Désirée-PVY^{NTN} interactions have focused on the detection of changes in the plant transcriptome and proteome, particularly those related to plant hormonal signaling (Baebler et al., 2011; Stare et al., 2015). Salicylic acid (SA) was found to be the crucial component for attenuation of the disease symptoms (Baebler et al., 2011). However, understanding of the mechanisms that underlie tolerance response to PVY^{NTN} is still incomplete.

RNA silencing is a basal antiviral system in plants, where DICER-like (DCL) proteins cleave viral dsRNA structures, giving rise to virus-derived small interfering RNAs (vsiRNAs), which are then incorporated into Argonaute (AGO) protein(s) to guide viral RNA degradation (Baulcombe, 2004). To counter this host defense mechanism, viruses have evolved viral suppressors of RNA silencing (Csorba et al., 2015). Helper component-proteinase (HCPro) of

potyviruses suppresses silencing by sequestering small RNAs (sRNAs) and AGO1 and thus counteracts the degradation of viral RNA (Ivanov et al., 2016). Another level of plant antiviral defense is mediated by resistance genes, leading towards effector triggered immunity, often resulting in hypersensitive response and programmed cell death (Zvereva and Pooggin, 2012; Coll et al., 2011). The cv. Désirée carries the *Ny* gene conferring resistance against strain PVY^{O}, but lacks resistance genes against the PVY^{NTN} strain (Singh et al., 2008) and thus does not respond by triggering an efficient effector triggered immunity.

Recent findings revealed that endogenous RNA silencing mediated by microRNAs (miRNAs) and small interfering RNAs (siRNAs) could play important roles in plant immunity (Seo et al., 2013; Navarro et al., 2005; Li et al., 2011; Weiberg and Jin, 2015). These 18-24-nt long non-coding sRNAs are able to negatively regulate gene expression by binding to the specific mRNA targets which leads to either promoting their degradation, inhibiting their translation, or suppressing transcription by epigenetic modification (Baulcombe, 2004; Chen et al., 2011; Wu et al., 2010; Chellappan et al., 2010). The endogenous RNA silencing can be amplified by the production of secondary phased siRNAs (phasiRNAs), triggered by 22-nt miRNAs/siRNAs (Chen et al., 2010; Cuperus et al., 2010). phasiRNAs are generated in phase relative to positions of the miRNA cleavage site, can be produced from both coding non-coding transcript (*PHAS* loci) and are able to target transcripts not only in *trans* but also their *PHAS* loci of origin in *cis* and thus additionally contribute to the autoregulation (Borges and Martienssen, 2015). miRNAs have been associated with defense responses against several pathogens (Peláez and Sanchez, 2013; Ruiz-Ferrer and Voinnet, 2009). Arabidopsis miR393 was the first plant miRNA reported to play a key role in antibacterial immunity by repressing auxin signaling (Navarro et al., 2005). Recently, several studies have uncovered the miRNA-mediated silencing of receptor gene (*R*-gene) transcripts. Infection by pathogens e.g. viruses or bacteria, relieves the silencing, leading to the accumulation of *R* proteins and activation of immune responses (Li et al., 2011; Shivaprasad et al., 2012; Park and Shin, 2015).

This growing body of evidence suggests that sRNAs are integral components of plant immunity. However, none of the studies performed so far investigated the sRNA regulatory network in potato-virus interaction at the systems level linking it to transcriptional regulation. The aim of this study was to investigate sRNAs' role in establishment of the tolerant response of potato to PVY^{NTN}, hence we have studied response in the early stage of viral infection,

before the viral multiplication can be detected. Employing high-throughput sequencing technology, we characterized and compared the sRNA expression patterns between PVY-infected and healthy tolerant potato plants. In addition, this information was linked with expression profiles of their target transcripts identified *in silico* and by Degradome-Seq and used for sRNA regulatory network construction. Besides the already described regulation of *R*-gene transcripts we have discovered a previously undescribed connection between sRNAs and gibberellin (GA) biosynthesis representing an important link between immune and developmental signaling pathways. This link was confirmed by hormonal content measurements. Additionally, we analyzed sRNA regulatory network in transgenic NahG-Désirée. We showed that response of the discovered sRNA network is attenuated when SA is deficient, indicating a mechanism through which SA is regulating disease tolerance in potato.

Results

Novel endogenous sRNAs identified in potato leaves

We identified 245 different previously described miRNAs (including 38 miRNA variants; isomiRs), belonging to 95 miRNA families in control and PVY^{NTN}-infected leaves of cv. Désirée using sRNA-Seq (**Supplemental Figure 1, Supplemental Dataset 1**). In addition, 141 novel miRNAs were detected, of those 12 were coded by multiple *MIR* loci. Novel miRNA sequences were assigned to 123 novel miRNA families (**Supplemental Dataset 1 and 2**).

When assessing the miRNA regulatory network, the amplification of silencing through phasiRNA biogenesis was also considered. In total, more than 4000 *PHAS* loci were predicted, coding for 2558 phasiRNAs. 124 loci were located on protein-coding regions of genes, with the majority encoding NBS-LRRs (nucleotide binding site-leucine rich repeat proteins) and LRR-RLKs (leucine rich repeat-receptor-like kinases) (**Supplemental Dataset 3 and 4**). Interestingly, several novel *PHAS* loci were discovered in coding regions of genes associated with stress signaling, such as *HSP70*, superoxide dismutase and auxin signaling F-box proteins (see **Supplemental Table 1** for the full list of genes used in this study together with their descriptions and corresponding IDs). We also confirmed that *StAGO1* is a *PHAS* locus (**Supplemental Dataset 3**), as previously described in Arabidopsis (Axtell et al., 2006).

We further compared miRNA expression profiles of PVY^{NTN}-infected versus mock inoculated leaves in early stages of virus infection (3 dpi, 1 day before detectable viral multiplication; (Baebler et al., 2011; Stare et al., 2015)). In total, 57 unique miRNAs were found to be significantly differentially expressed in early stages of PVY^{NTN} infection (3 dpi) of Désirée plants. Virus infection predominantly caused an increase in miRNAs levels (**Supplemental Dataset 1**). Additionally, we identified 35 phasiRNAs as differentially regulated 3 dpi, mainly originating from noncoding *PHAS* and *NBS-LRR* loci (**Supplemental Dataset 4**). To validate the obtained sRNA-Seq results, abundance of six differentially expressed miRNAs was analyzed by stem-loop RT-qPCR. As shown in (**Supplemental Figure 2,** all sRNA-Seq differential expression results were confirmed.

In previous studies, a plethora of potato miRNA/phasiRNAs have been shown to be differentially expressed following pathogen infection. However, the biological relevance of these differences remains largely unknown. To translate the data obtained on sRNA level into changes in physiological processes, we performed *in silico* sRNA target prediction, both at the levels of translational inhibition and target cleavage (**Supplemental Dataset 5**). Additionally, the predictions of target cleavage were experimentally validated by Degradome-Seq (**Supplemental Dataset 6**). Based on this information we constructed a potato sRNA regulatory network connecting miRNAs with phasiRNAs and their targets (**Supplemental Online File 1 and 2**). This revealed several already known and many novel connections linking sRNA regulation to the plant immune signaling (see example in **Supplemental Figure 3; Supplemental Dataset 5 and 6**). Several miRNA-mRNA pairs conserved across plant species, such as miR156-*SPL11*, miR160-*ARF10*, miR172-*AP2* or miR396-*GRF5* (Curaba et al., 2014), were confirmed also in our system (**Supplemental Dataset 5 and 6)**. Our data also showed the miR393-mediated cleavage of transcripts encoding members of *TIR/AFB* gene family, receptors implicated in the control of auxin signaling (**Figure 1**) (Si-Ammour et al., 2011). We also discovered that these transcripts were targets of several *TIR1*-derived phasiRNAs (phasiTIRs) (**Figure 1, Supplemental Dataset 5 and 6**) (Si-Ammour et al., 2011). Moreover, we identified that the miR393- and phasiTIR-network is also targeting downstream transcription factor StARF1 and other phytohormone signaling pathways, such as transcripts involved in ethylene signaling (*StERF2a, StAP2*, and *StEIN4*), in jasmonate signaling (*StLOX1* and *StOPR1*) and in brassinosteroid biosynthesis (*StDWF4*) (**Figure 1,**

Supplemental Dataset 5 and 6) indicating much larger complexity of sRNA network regulation as so far predicted.

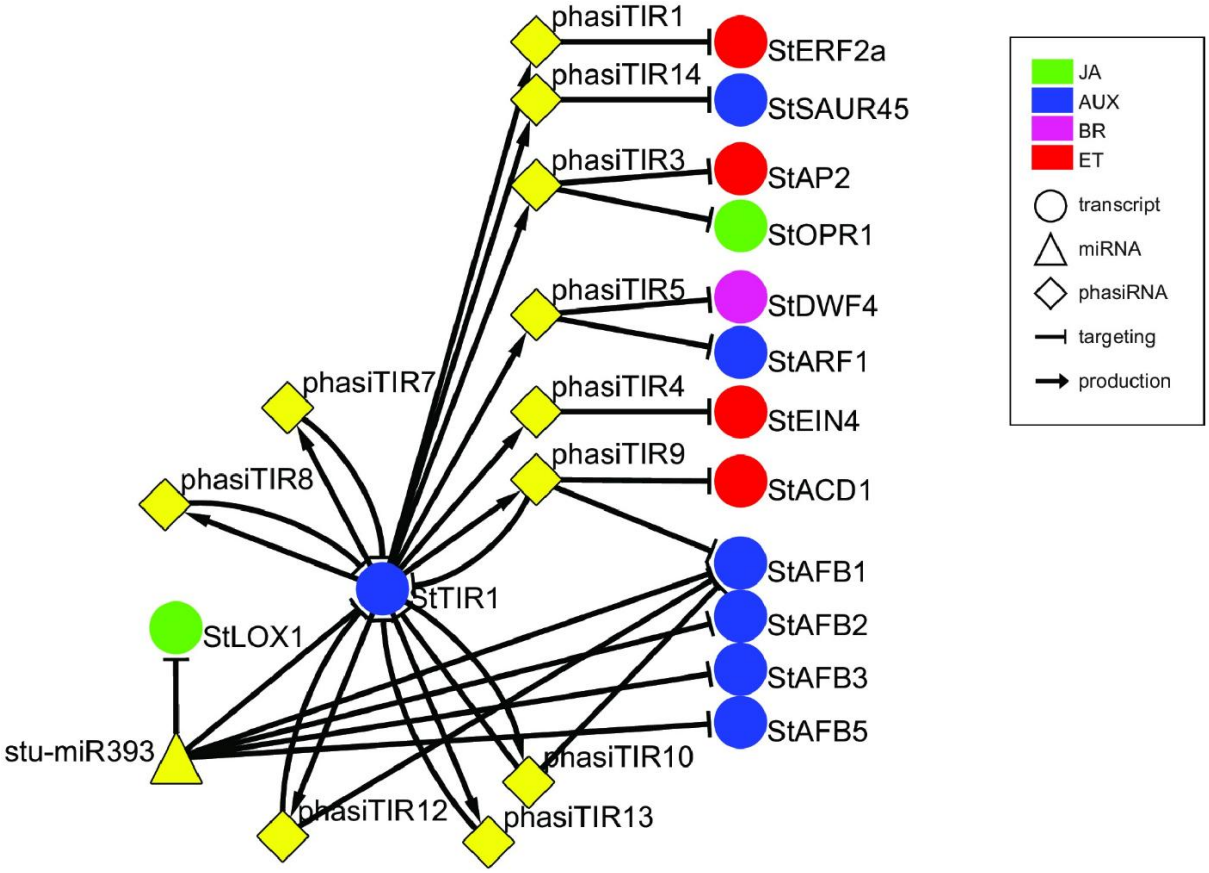

Figure 1. **miR393-mediated cleavage of StTIR1 leads to production of phasiTIRs targeting diverse phytohormone signaling components**. Node shapes represent classes of sRNAs (triangle – miRNA; diamond – phasiRNA) or transcripts (circle). Node colors indicate components related to different hormone signaling pathways: green – jasmonic acid (JA); blue – auxin (AUX); magenta – brassinosteroid (BR); red – ethylene (ET). Arrows connect sRNAs and targets (blunt-end arrow) or *PHAS* loci and producing phasiRNAs (regular arrow). Node stu-miR393 represents miR393-5p and miR393-5p.1 and node StAFB1 represents StAFB1.1, StAFB1.2, and StAFB1.3. For details of the target transcripts/genes see **Supplemental Table 1**. StTIR1 – Transport inhibitor response 1, StLOX1 – Lipoxygenase 1, StERF2a – Ethylene responsive transcription factor 2a, StSAUR45 – Small auxin upregulated RNA 45, StAP2 – APETALA2, StOPR1 – 12-oxophytodienoate (OPDA) reductase, StDWF4 – Dwarf4, StARF1 – Auxin response factor 1, StEIN4 – Ethylene insensitive 4, StACD1 – 1-aminocyclopropane-1-carboxylic acid deaminase 1, StAFB1/2/3/5 – Auxin F-box 1/2/3/5.

We also found that the vast majority of differentially expressed miRNAs and phasiRNAs targets encode defense related proteins such as pathogenesis-related (PR) proteins and proteins involved in the biosynthesis of secondary metabolites, transcription factors belonging to AP2/ERF, bHLH, MYB and GRAS family proteins, putative immune receptors (NBS-LRRs, LRR-RLKs) as well as proteins involved in biosynthesis and signaling of different phytohormones (**Figure 2A**).

184

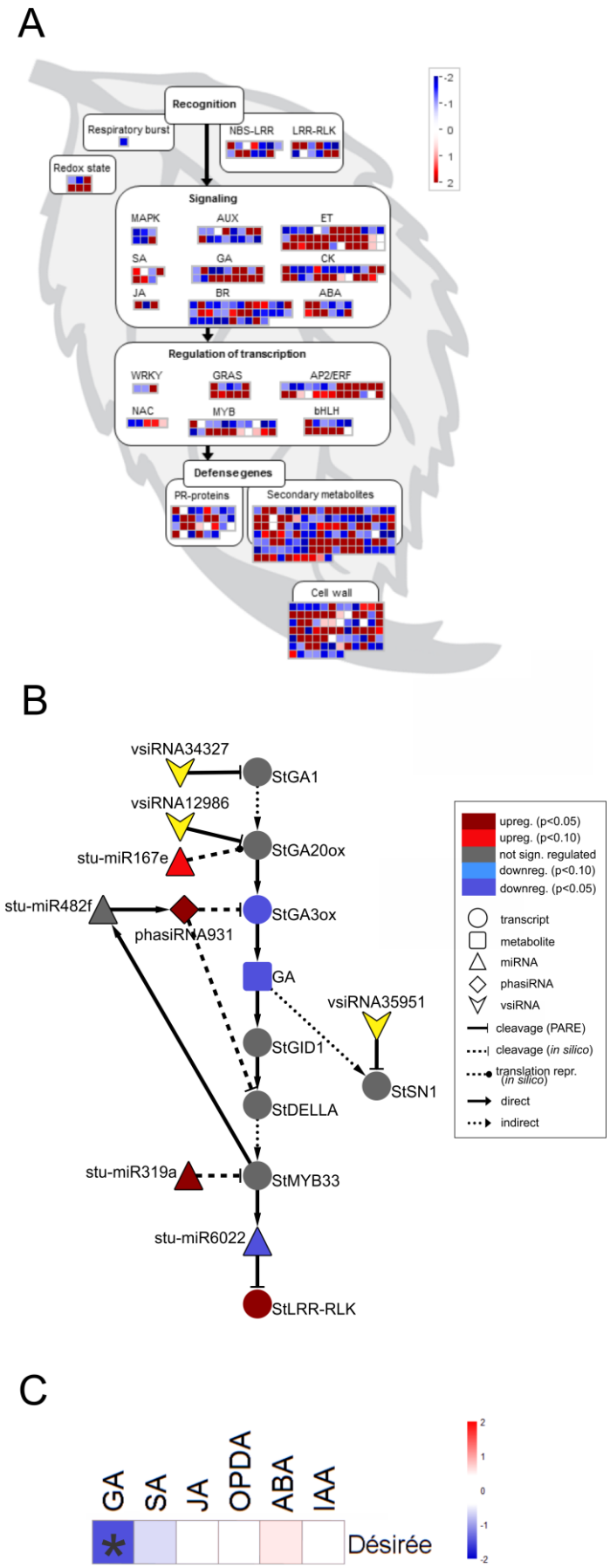

185

Figure 2. PVY induced changes in sRNA regulatory network are controlling multiple immune and gibberellin signaling components in Désirée at the onset of viral multiplication. (**A**) Visualization of differentially expressed miRNAs/phasiRNAs in PVY^{NTN}-infected Désirée according to the function of their targets. Each square represents log_2 ratios of expression between PVY^{NTN}- and mock-inoculated plants (red – upregulated; blue – downregulated). MapMan ontology bins: respiratory burst (20.1.1), redox state (21.6), MAPK (30.6), SA (17.8), JA (17.7), AUX (17.2), GA (17.6), BR (17.3), ET (17.5), CK (17.4), ABA (17.1), WRKY (27.3.32), NAC (27.3.27), GRAS (27.3.21), MYB (27.3.25), AP2/ERF (27.3.3), bHLH (27.3.6), PR-proteins (20.1.7), secondary metabolites (16), cell wall (10). The NBS-LRR and LRR-RLK bins were custom constructed for this study, based on their harboring domains (obtained from PFAM database; (Finn et al., 2016)). These bins represent differentially expressed miRNAs/phasiRNAs targeting NBS-LRRs or LRR-RLKs. NBS-LRR – nucleotide binding site-leucine-rich repeat protein, LRR-RLK – leucine-rich repeat receptor-like kinase, MAPK – mitogen activated protein kinase, SA – salicylic acid, JA – jasmonic acid, AUX – auxin, GA – gibberellin, BR – brassinosteroid, ET – ethylene, CK – cytokinin, ABA – abscisic acid, PR – pathogenesis-related. (**B**) Network of differentially expressed endogenous sRNAs and vsiRNAs targeting mRNAs of GA biosynthesis and signaling pathways in Désirée 3 days post PVY^{NTN} inoculation. Node shape represent classes of sRNAs (triangle – miRNA; diamond – phasiRNA; arrowhead – vsiRNA), transcripts (circle) or metabolites (rectangle). Statistical significances of expression differences (p-values) and direction of expression change are represented by the node colors (see the legend). Arrows indicate type of interaction (solid-line normal arrow – direct interaction; dashed-line normal arrow – indirect interaction; blunt-end solid arrow – cleavage observed by Degradome-Seq, blunt-end dashed-line arrow – *in silico* predicted cleavage (or translational repression as proposed by Rogers and Chen (Rogers and Chen, 2013), dashed-line oval arrow – *in silico* predicted translational repression). Node stu-miR319a represents stu-miR319a-3p, stu-miR319a-3p.2, stu-miR319a-3p.4 and stu-miR319b-3p. Node StGA20ox represents StGA20ox, StGA20ox1, StGA20ox3 and StGA20ox4. For details of the target transcripts/genes see **Supplemental Table 1**. Stu-miR167e – stu-miR167e-3p; stu-miR482f – miR482f-3p; stu-miR6022 – miR6022-3p; StGA1 – GA REQUIRING 1 (ent-copalyl diphosphate synthase); StGA20ox – GA20-oxidase; StGA3ox – GA3-oxidase; StGID1C – GA receptor - GA INSENSITIVE DWARF1C hydrolase; StSN1 – Snakin-1; StDELLA – DELLA protein; StLRR-RLK – leucine-rich repeat receptor-like protein kinase. (**C**) Changes in concentrations of a set of plants hormones in Désirée 3 days after PVY^{NTN} infection. sRNA-mediated repression of GA biosynthesis was confirmed by reduced GA_3 levels in PVY-infected Désirée plants**.** Colors present as log_2 ratios of mean concentrations between PVY^{NTN}- and mock-inoculated plants (n=4; red – increased, blue – decreased level). * - indicate statistically significant values (ANOVA; $p < 0.05$). SA – salicylic acid, JA – jasmonic acid, OPDA –12-oxophytodienoic acid, ABA – abscisic acid, IAA – indole-3-acetic acid.

sRNA regulatory network reponse in tolerant interaction resemble responses in mutualistic symbiosis

Analysis of the differentially expressed miRNAs and phasiRNAs together with the levels of the target transcripts (data published in (Stare et al., 2015)) revealed the presence of many known, as well as novel, regulatory cascades involving *NBS-LRR*s. Several *NBS-LRR*s were predicted to be targeted by miR482, miR6024 and miR6027 family members (**Supplemental Dataset 5 and 6**). Moreover, *NBS-LRRs* are regulated also by phasiRNAs, where most phasiRNAs have multiple *NBS-LRR* targets (**Supplemental Figure 4**, **Supplemental Dataset 5 and 6**) due to the shared conserved P-loop or Walker A motif (Shivaprasad et al., 2012). In all of the previous studies miR482 family members were downregulated following pathogen infection (Ouyang et al., 2014; Shivaprasad et al., 2012; Yang et al., 2015). In our study, however, the one regulated member of the miR482 family (miR482e) targeting *NBS-LRR* transcripts was upregulated following PVY^{NTN} infection (**Supplemental Dataset 1**), similarly

as observed in establishment of mutualistic symbiosis in soybean roots (Li et al., 2010). Moreover, several miRNAs that were upregulated in response to PVY^{NTN} in cv. Désirée, such as miR164, miR167, miR169, miR171, miR319, miR390, miR393, miR397 and miR398 have also been reported to regulate nodulation and arbuscular mycorrhizal symbiosis in different legume species (**Supplemental Dataset 1**; (Mao et al., 2013; Yan et al., 2015; Lelandais-Brière et al., 2009; De Luis et al., 2012; Devers et al., 2011). In addition to NBS-LRR proteins, LRR-RLKs are also important mediators of immune as well as important triggers of mutualistic symbiosis signaling cascades (Hohmann et al., 2017; Antolin-Llovera et al., 2014). We have identified a novel miRNA-LRR-RLK interaction in which miR6022 levels decrease in response to PVY^{NTN} infection in cv. Désirée, which is further linked to upregulation of its predicted target genes encoding LRR-RLKs (**Supplemental Figure 4A**).

Several PVY^{NTN}- derived siRNAs trigger degradation of host transcripts

The primary plant defense mechanism against invading viruses is RNA silencing involving the production of vsiRNAs. The population of vsiRNAs detected in the infected samples consisted of more than 46 000 unique sequences of 20-24 nt in length (**Supplemental Dataset 7**). In order to take into account the unlikely possibility that PVY^{NTN} produces its own miRNAs, we first ran the miRNA prediction pipeline on vsiRNAs and the viral genome. However, we found no sequence that would fullfill the criteria for a viral miRNA. Subsequently, we searched for potential host transcripts targeted by vsiRNAs in our experimentally validated target degradation dataset (**Supplemental Dataset 8**). We found that vsiRNAs are indeed able to target multiple potato transcripts, among them mRNAs coding for immune receptor proteins, various transcription factors and proteins involved in hormonal signaling pathways (**Supplemental Dataset 8)**. For example, several vsiRNAs were detected with the confirmed ability to guide the cleavage of transcripts involved in auxin signaling, transcripts encoding IAA-amino acid hydrolases (StILR1 and StIAR3), Aux/IAA transcriptional repressors (StIAAs) and the transcription factor StARF2.

sRNA-mediated downregulation of GA biosynthesis genes is reflected in lower GA_3 levels

Interestingly, we found that GA biosynthesis and downstream signaling are targeted by a sRNA-mediated regulatory network and that the changes in sRNA levels following PVY^{NTN} infection are reflected also in the changes of their target transcripts levels (**Figure 2B,**

Supplemental Dataset 5). GA20-oxidase (GA20ox) and GA3-oxidase (GA3ox) are enzymes that catalyze the last steps in the formation of bioactive GAs (Yamaguchi, 2008). We found that in Désirée plants the *StGA20ox* transcript is regulated by miR167e (**Figure 2B**). An additional layer of GA biosynthesis regulation is represented by increased production of phasiRNA931, which promotes cleavage of the *StGA3ox* transcript. The transcriptomics results support these interactions as the targeted transcripts are significantly downregulated in Désirée upon PVY^{NTN} infection (**Figure 2B, Supplemental Dataset 5**). Additionally, vsiRNAs were found to target transcripts encoding two enzymes involved in GA biosynthesis *StGA1 and StGA20ox* (**Figure 2B, Supplemental Dataset 8**). One also has to note that all of the miRNAs/phasiRNAs discovered to be involved in sRNA-GA biosynthesis regulation have so far not been identified in Arabidopsis and among them only miR167e was also discovered in tomato (Griffiths-Jones et al., 2006; Zhang et al., 2014).

Downstream GA signaling is also targeted by sRNAs in the potato-PVY interaction on multiple levels. The four miR319 family members were predicted to cleave the transcript encoding StMYB33, a GA-induced MYB-like transcription (GAMYB) factor orthologue (Millar and Gubler, 2005), whereas phasiRNA931 targets a potato orthologue of a DELLA protein, a GA-signaling repressor (**Figure 2B**).

Such interconnectedness between plant defense related miRNA/phasiRNA network and GA biosynthesis/signaling has not been previously identified and may represent a link between defensive and developmental signaling. Thus, we decided to functionally evaluate these results by measuring the concentrations of a set of plant hormones. As predicted by the sRNA-target transcript analyses, we detected a reduced level of GA_3 in PVY^{NTN} infected Désirée plants (**Figure 2C**). The levels of SA, jasmonic acid (JA), the JA precursor 12-oxophytodienoic acid (OPDA), abscisic acid (ABA) and indole-3-acetic acid (IAA) remained unchanged at 3 dpi (**Figure 2C, Supplemental Dataset 9**). To inspect if GA deficiency has any impact on plant growth, plants height was monitored till 21 dpi. No differences were observed between all four studied groups of plants.

The miRNA regulatory network and transcriptional regulation are tightly interconnected

Given the critical role of miRNAs in gene regulation, *cis*-regulatory elements of differentially expressed *MIR* genes involved in *R*-gene regulation and GA signaling were investigated.

Interestingly, GAMYB binding sites were detected in the promoters of the *MIR6022* and *MIR482f* genes (**Supplemental Dataset 10**). Moreover, these genes harbor WRKY8/28/48 binding sites, while *MIR319a* harbors a general WRKY binding W-box regulatory element. Additionally, *cis*-acting elements involved in SA and JA responsiveness were identified in the promoters of the *MIR482f* gene. In all three analyzed promoter sequences for NAC transcription factor binding sites were detected (**Supplemental Dataset 10**). The promoter of *MIR167e* is only partially assembled in the current version of the potato genome; thus, the promoter analysis was performed only for the first 80 nt upstream of the predicted hairpin precursor sequence (**Supplemental Dataset 10**).

SA depletion attenuates sRNA response following PVY^{NTN} infection

As the link between repression of GA signaling and disease symptoms severity was already established in Arabidopsis (Du et al., 2014) we have further investigated the activity of discovered sRNA-GA circuit in susceptible potato-PVY^{NTN} interaction. We have shown previously that SA depletion breaks the equilibrium between disease and tolerance. In NahG-Désirée plants the pronounced disease symptoms appeared both on the inoculated and systemic leaves (Baebler et al., 2011). Furthermore, the viral multiplication was detected 1 day earlier than in non-transgenic Désirée plants (at 4 dpi), while the final concentrations of the virus were not significantly higher (Baebler et al., 2011). Here, we performed the analysis of sRNA response as well as the measurements of hormonal concentrations in interaction of this susceptible genotype with the virus. Interestingly, we found that the overall response of sRNAs was attenuated in NahG-Désirée at 3 dpi. In NahG-Désirée only 20 miRNAs were differentially expressed, with the majority showing a lower degree of induction than in Désirée plants (**Figure 3 and 4A, Supplemental Dataset 1**).

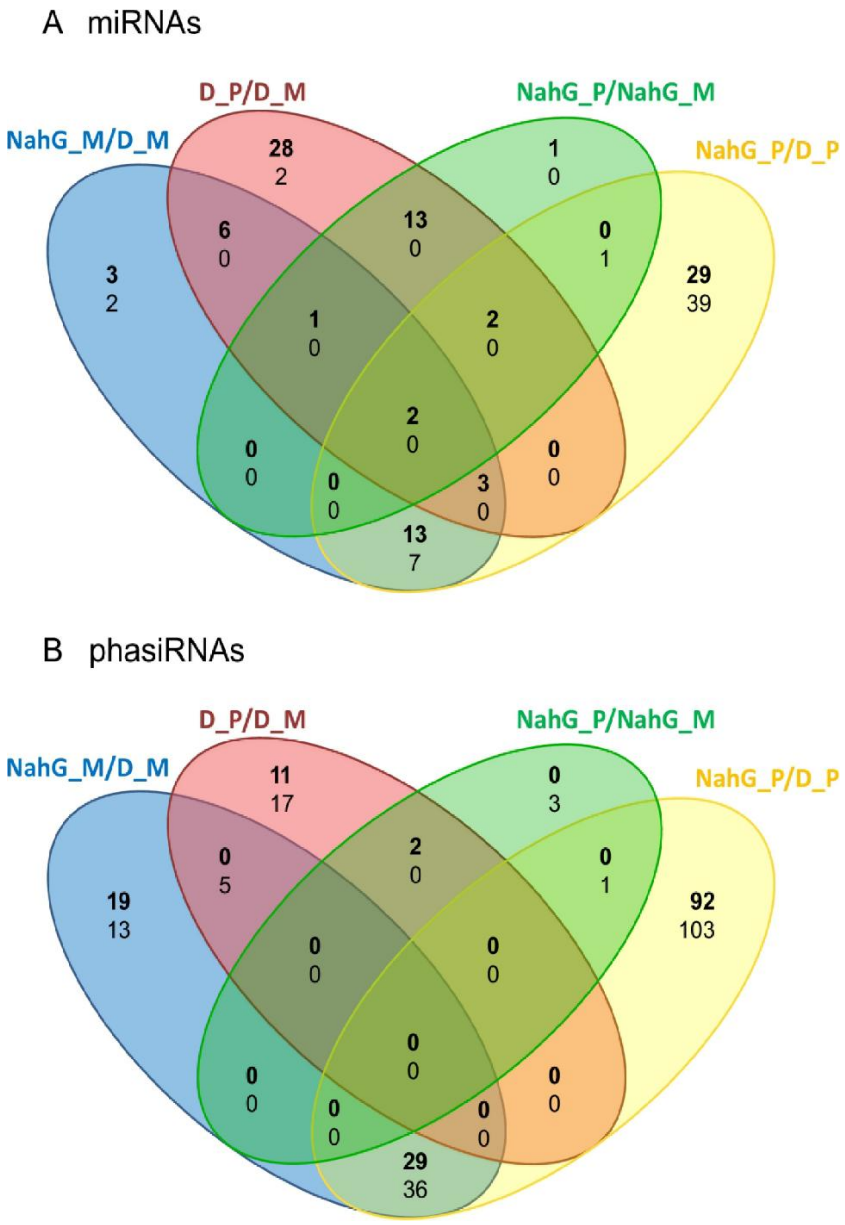

Figure 3. Numbers of unique and common differentially expressed miRNAs and phasiRNAs 3 days post PVY^{NTN} inoculation in comparison of SA-deficient and nontransgenic Désirée plants. Venn diagrams show the number of differentially expressed (FDR corrected p-value < 0.05) (**A**) miRNAs and (**B**) phasiRNAs in mock- or PVY^{NTN}-inoculated potato leaves of cv. Désirée and NahG-Désirée. Upregulated miRNAs/phasiRNAs are shown in bold and downregulated in normal text. D – Désirée, NahG – NahG-Désirée, M – mock, P – PVY^{NTN}.

Inspecting specifically the discovered link between sRNAs regulation, GA signaling and immune signaling in the sRNA and transcriptional datasets we observed that the responses of miR167e and miR319a are diminished in NahG-Désirée plants (**Figure 4B**, **Supplemental Dataset 1**). Interestingly, although the phasiRNA931 was also upregulated in NahG-Désirée plants, albeit to a lower extent, this was not translated into downregulation at the target transcript level (**Figure 4B, Supplemental Dataset 5**). Adding to the significance of this finding, in NahG-Désirée plants the level of bioactive GA was not significantly different in

339 infected leaves (**Figure 4C**). Furthermore, the relieved silencing of LRR-RLKs by miR6022
340 that is predicted to modulate immune response and which is also linked with GAMYBs was
341 absent in NahG-Désirée plants (**Supplemental Figure 4B**). We also inspected sRNA-
342 mediated responses which resembled responses in mutualistic symbioses in tolerant plants of
343 Désirée and found that miR482e was also upregulated in NahG plants, while regulation of
344 miR164, miR167, miR169, miR171, miR319, miR390, miR393, miR397, miR398, was
345 diminished (**Supplemental Dataset 1**).
346

A

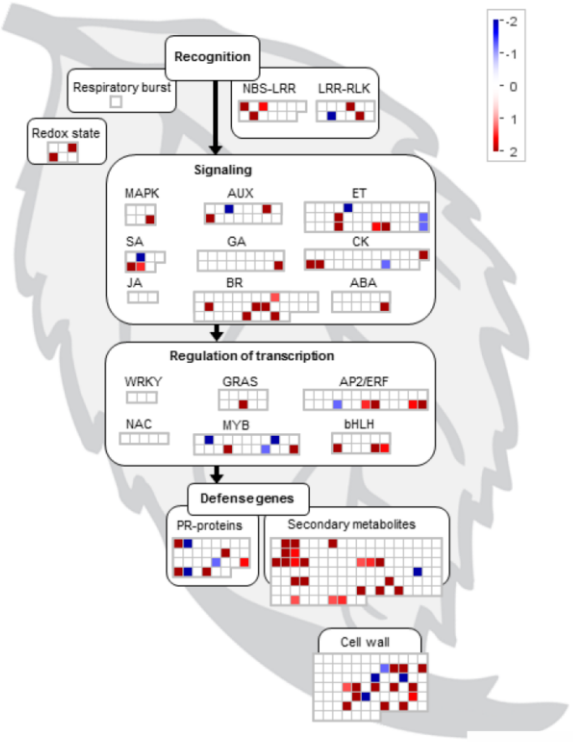

B

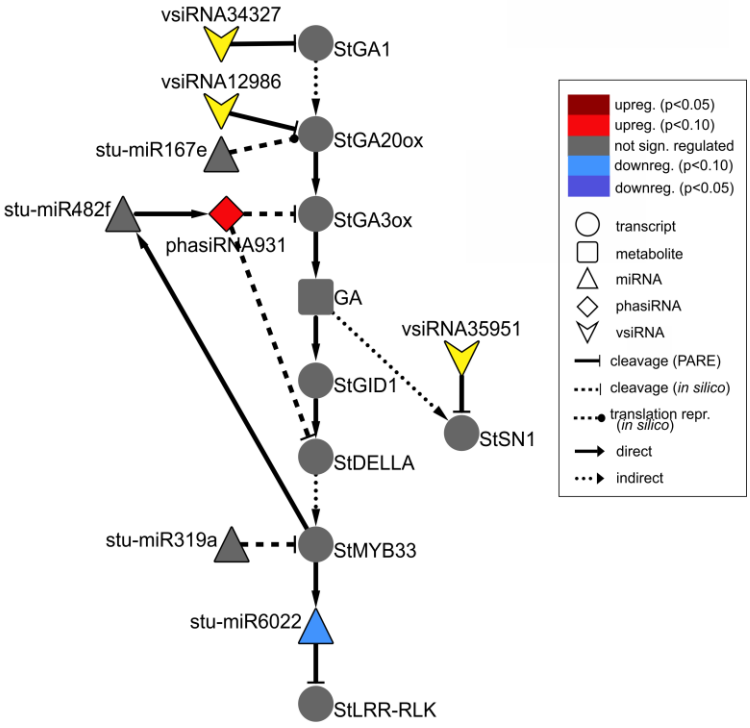

C

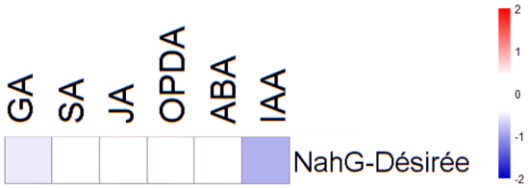

Figure 4. sRNA response is attenuated in susceptible SA depleted plants following PVY^{NTN} infection. (**A**) Visualization of differentially expressed miRNAs/phasiRNAs in PVY^{NTN}-infected NahG-Désirée according to the function of their targets. Each square represents $\log_2$ ratios of expression between PVY^{NTN}- and mock-inoculated plants (red – upregulated; blue – downregulated). (**B**) Network of endogenous sRNAs and vsiRNAs targeting mRNAs of GA biosynthesis and signaling pathways in NahG-Désirée 3 days post PVY^{NTN} inoculation. (**C**) Concentrations of a set of plants hormones in NahG-Désirée 3 days after PVY^{NTN} infection. The levels of all analyzed hormones remained unchanged in NahG plants following PVY^{NTN} infection. Colors present as $\log_2$ ratios of mean concentrations between PVY^{NTN}- and mock-inoculated plants (n=4; red – increased, blue – decreased level). * - indicate statistically significant values (ANOVA; $p < 0.05$). For abbreviations and other details of the scheme, see the caption of **Figure 2**.

To evaluate the direct effect of the SA deficiency in NahG plants, independently of the viral infection, we also compared the sRNA expression profiles in mock-inoculated leaves of non-transgenic and SA-depleted Désirée (**Figure 3**). We found 37 miRNAs regulated by SA. It seems that SA in the normal growing conditions generally causes the reduction in the level of miRNAs as majority (28) of miRNAs were detected at significantly higher levels in NahG-Désirée plants (**Supplemental Dataset 1**). When we similarly compared the expression profile of transcripts between the two genotypes we detected that the most strongly induced by SA signaling are notably different WRKY transcription factors (**Table 1, Supplemental Dataset 11 and 12**), among them orthologues of Arabidopsis *WRKY70,* which was already shown to be positively regulated by SA (Li et al., 2004). As *MIR319a* and *MIR482f* promoters are regulated by WRKY transcription factors (**Supplemental Dataset 10**), we discovered a direct link between SA signaling and miRNA regulatory network in potato.

Discussion

We hypothesized that fine-tuned regulation of subsets of genes involved in defensive signaling can interfere with developmental signaling, which could explain decreased symptom severity in plants expressing tolerance to virus infection. The sRNAs have proven to be an important level for precise regulation of several developmental processes. We here show that the integration of sRNA network and transcriptional regulation is also crucial in entanglement of immune responses and developmental processes.

Integration of the sRNA regulatory network with sRNA expression and expression profiles of their targets confirmed many known, but also revealed several novel regulatory circuits associated with immunity regulation and hormone signaling (**Figure 1 and 2, Supplemental Figure 3 and 4, Supplemental Dataset 5 and 6).** When plants are exposed to pathogens,

NBS-LRRs and LRR-RLKs are the key players in sensing and transducing stress signals (Jones and Dangl, 2006; Antolin-Llovera et al., 2014). Viral suppressors of silencing can release the tight control of *R*-gene silencing by sRNAs and activate immune responses in plants (Shivaprasad et al., 2012; Li et al., 2011). Our study investigated regulatory processes occurring early after infection, before virus concentration significantly increased thus the effects we detected were not caused by extensive HCPro or any other viral protein accumulation. Even so, we have detected diverse regulation of NBS-LRRs and LRR-RLKs and their targeting miRNAs as expected according to their specialized roles (**Supplemental Figure 4)**. On the other hand, similarity of response between mutualistic symbiosis in legumes and tolerance in potato was shown by the miR6022-relieved silencing of LRR-RLKs as well as by profiles of several other miRNAs (**Supplemental Figure 4A**, **Supplemental Dataset 1**; (Mao et al., 2013; Yan et al., 2015; Lelandais-Brière et al., 2009; De Luis et al., 2012)). This suggests a similar sRNA network modulation of immune response and physiology occurs in both mutualistic and disease tolerant (commensalistic) interactions. In tolerance, plants may adopt some processes resembling mutualistic symbiosis to control plant response and minimize severe disease symptoms allowing non-hindered development of the plant and at the same time multiplication of the virus.

Phytohormones modulate plant defense responses against various biotic and abiotic stresses as well as plant growth and development (Huot et al., 2014). Till now, several miRNAs were confirmed to participate in this complex network, mainly in connection to repression of auxin signaling (Navarro et al., 2005). A similarly complex miR393/miR396/phasiTIR auxin signaling network was identified in this study, yet showing links also to other hormonal signaling pathways (**Figure 1, Supplemental Figure 3**).

Most notable is, however, the novel link between sRNA regulatory network and GA biosynthesis and signaling. Biotic stress was shown to repress GA signaling pathways (Wang et al., 2007). Here, we show that GA biosynthesis and signaling are post-transcriptionally regulated via multiple miRNAs, phasiRNAs as well as vsiRNAs in potato leaves following infection with PVY^{NTN} (**Figure 2B**). The effect of this regulatory circuit was confirmed by reduced bioactive GA level in the tolerant Désirée plants (**Figure 2C**). This reduction was however not reflected in decreased plant growth and was thus most probably transient and localized in nature (Karasov et al., 2017). In other plant species, GA biosynthesis was shown to be indirectly targeted by miRNAs regulating the activity of the corresponding

418 transcription factors (miR319-TCP14-GA2ox/GA20ox; miR393-GRF2-GA3ox/GA20ox)
419 (Curaba et al., 2014), while direct interactions were to our knowledge not yet reported.
420 Also of note, the sRNAs regulating GA biosynthesis identified here were not identified in
421 Arabidopsis and seem to be Solanaceae specific.
422
423 Moreover, downstream GA signaling components are affected by the sRNA regulatory
424 network as well. *StMYB33*, an orthologue of Arabidopsis GAMYB proteins, *MYB33*, is
425 regulated by miR319a, a close relative of miR159 (Palatnik et al., 2007). The two
426 Arabidopsis *GAMYBs* were shown to be regulated by miR159 (Allen et al., 2007). The
427 functional relation between lower activity of GA signaling was already directly confirmed to
428 be related to disease severity in three different experimental systems. Arabidopsis *GAMYB*
429 double knockout showed ameliorated symptoms when infected with *Cucumber mosaic*
430 *virus* (CMV) (Du et al., 2014), similarly was shown in rice in interaction with bacteria
431 (*Xanthomonas oryzae* pv. *oyrzae*) and fungi (*Magnaporthe oryzae*) using knockout in GA
432 deactivating enzyme (Yang et al., 2008). Also in line with this, decrease in GA levels and
433 increase in DELLA protein concentrations was shown to trigger components of rhizobial
434 and mycorrhizal signaling (Jin et al., 2016; Fonouni-Farde et al., 2016; Calvo et al., 2004;
435 Ghachtouli et al., 1996; Floss et al., 2013), showing yet another similarity between tolerant
436 response of potato to viral infection and response of plants in mutualistic symbiosis.
437
438 With the discovery of GAMYB binding sites in the *MIR482f* and *MIR6022* promoters
439 (**Supplemental Dataset 10)**, we found the circuit in sRNA-GA signaling and additionally a
440 link between GA signaling and *R*-gene expression. The complexity of regulatory responses
441 observed in this study (**Figure 5**) is in line with the systems biology paradigm that interaction
442 of multiple components and not a single component within a cell leads to much of biological
443 function (Westerhoff et al., 2015). Although the reductionist approach is powerful in building
444 logically simple hypotheses and devising ways to test them, it is very difficult to reconstitute
445 the function for a whole biological system based solely on that as the behavior of the system
446 may depend heavily on complex interactions within the system (Katagiri, 2003). Thus, we
447 have adopted a systems level confirmation of our hypothesis that sRNA-GA-immune
448 signaling circuit is important for establishment of tolerant interaction. Previously, we had
449 demonstrated that SA regulates plant responses to virus infection; not only by delaying viral
450 multiplication, but also by controlling disease symptom severity, most probably via its effects

on host primary metabolism (Baebler et al., 2011). In this study we have confirmed that response of sRNA regulatory networks controlling potential immune receptors and hormonal signaling is strongly attenuated in the NahG-transgenic plants in the early stage of viral infection (3 dpi; **Figure 3 and 4)** showing the role of sRNAs in linking immune signaling and symptomology. The molecular mechanisms of the link between SA signaling and sRNA network are also complex. SA has been shown to induce *RNA-dependent RNA polymerase 1* expression, which is crucial for the maintenance of basal resistance to several RNA viruses (Carr et al., 2010; Yu et al., 2003) but none of the silencing mechanism related enzymes are regulated in SA deficient NahG-Désirée plants (**Supplemental Dataset 11;** (Stare et al., 2015)). We have here predicted and experimentally confirmed SA-directed transcriptional regulation of *MIR482f*, the miRNA linking the GA signaling circuit and *R*-gene expression (**Figure 5, Supplemental Dataset 1 and 10)**, which could be additional link between SA signaling and symptoms development in potato-PVY interaction. An additional link are the WRKY transcription factors that are under positive control of SA (**Table 1**, **Supplemental Dataset 11 and 12**) and were predicted to regulate promoters of all three miRNAs involved in sRNA-GA circuit (**Figure 5, Supplemental Dataset 10**).

The outcome of plant-pathogen interactions depends on the delicate balance between plant immune signaling network and its interaction with pathogen. Here, we focused on the roles of sRNA networks in establishment of the tolerance to PVY infection. We showed that the sRNA regulatory network links immune and developmental signaling in potato through newly discovered sRNA-GA circuit. Tolerance of potato to virus infection perturbs sRNA network resulting in downregulation of GA-mediated signaling, as well as modulation of *R*-gene transcript levels; this results in amelioration of disease symptoms. Supporting this, the responses observed for individual miRNAs are similar as observed in establishment of mutualistic symbioses. It is thus plausible that a similar modulation of plant responses occurs in both mutualistic symbiosis and tolerance. This is in line with growing evidence showing that viruses, like other symbionts, lie on a continuum between antagonistic and mutualistic relationships (Roossinck, 2015; Kamitani et al., 2016).

Methods

Plant material

Potato leaves of cv. Désirée were mock or PVY^{NTN}-inoculated (isolate NIB-NTN, GenBank accession no. AJ585342) as described previously (Stare et al., 2015). Plant material of the inoculated leaves was collected 3 days post inoculation (dpi, corresponding to early stages of viral multiplication in both genotypes and before symptoms development in NahG-Désirée plants) for each treatment. Three and four biological replicates (individual leaves from different plants per group) were analyzed for RNA analysis and for hormonal measurements, respectively. Three plants from each group were monitored for plant height, till 21 dpi, when they all started to senesce. The same experimental set up was designed also for analysis of transgenic NahG-Désirée plants (Halim et al., 2004).

RNA extraction, library preparation and sRNA sequencing

Total RNA was extracted from 100 mg of homogenized leaf tissue using TRIzol reagent (Thermo Fisher Scientific, Waltham, MA) and MaXtract High Density tubes (Qiagen, Hilden, Germany) following manufacturers' protocols. RNA concentration, quality and purity were assessed using agarose gel electrophoresis and NanoDrop ND-1000 spectrophotometer (Thermo Scientific). sRNA NGS libraries were generated from total RNA samples using the TailorMix miRNA Sample Preparation Kit (SeqMatic LLC, Fremont, CA) and sequenced on the Illumina HiSeq 2000 Sequencing System at SeqMatic LLC.

Identification of endogenous and virus-derived sRNAs

The raw reads were quality filtered using Filter Tool of the UEA sRNA Toolkit (Moxon et al., 2008) by discarding low complexity reads (containing at most two distinct nucleotides), reads shorter than 18 nt and longer than 25 nt, reads matching tRNA/rRNA sequences and reads not mapped to the potato genome (PGSC_DM_v4.3) (Xu et al., 2011). To identify known annotated miRNAs, the remaining reads were compared to all plant miRNAs registered in miRBase database (release 21) (Kozomara and Griffiths-jones, 2014), allowing no mismatches. The sequences that matched mature miRNAs from other plants than potato (miRNA orthologs), were mapped to the potato genome to find corresponding *MIR* loci able

to form hairpin structure (An et al., 2014) and named according to annotation of conserved miRNA (Meyers et al., 2008). miRNAs that had different 5′ and 3′ ends with respect to the mature miRNA, were annotated as isomiRs. To identify novel unannotated miRNAs, filtered reads were submitted to miRCat tool of the UEA sRNA Toolkit using default parameters for plants, considering only reads of lengths 18-24 nt. Reads were first mapped to the potato genome, then the 100 and 200 nt long windows around the aligned reads were extracted (An et al., 2014). The predicted secondary structures were trimmed and analyzed to verify the characteristic hairpin pre-miRNA structure according to plant miRNAs annotation criteria (Meyers et al., 2008). An additional criterion we have imposed was that novel miRNAs should be present at least in two analyzed samples with more than five raw reads. Potential novel miRNAs were mapped against miRBase and sequences that matched known plant miRNAs with up to three mismatches were excluded. The novelty of potato specific miRNAs was verified with the miRPlant version 5 (An et al., 2014) using default parameters and additionally rechecked against the latest releases of Rfam (Nawrocki et al., 2015); http://rfam.xfam.org/), tRNA (Chan and Lowe, 2016); http://gtrnadb.ucsc.edu/) and snoRNA databases (Yoshihama et al., 2013); http://snoopy.med.miyazaki-u.ac.jp/). Families of novel miRNAs were determined by clustering their sequences with sequences of known miRNAs using CD-HIT with identity threshold of 0.9 (Huang et al., 2010). To identify vsiRNAs, reads of lengths 20-24 nt from all PVY^{NTN}-infected samples were mapped to the reconstructed consensus PVY^{NTN} genome (Kutnjak et al., 2015) using CLC Genomics Workbench version 8 (http://www.clcbio.com/) allowing only 100 % identity.

Prediction of novel potato phasiRNAs and *PHAS* loci

Prediction of phasiRNAs and phasiRNA-producing loci (*PHAS* loci) was performed using ta-siRNA prediction tool (Chen et al., 2007) utilizing the potato genome (Xu et al., 2011) and the merged potato gene and unigene sequences StNIB_v1 (Ramšak et al., 2014). To detect *PHAS* loci with a significant degree of phasing ($p < 0.0001$) and to investigate whether phasing also occurs in sRNAs with phase sizes different from 21 nt, different phasing intervals ranging from 21 to 24 nt were analyzed.

sRNA quantification and statistical analysis

Differential expression analysis was performed in R (R development Core Team, 2011; version 3.2.2), using the limma package (Ritchie et al., 2015). In short, sRNA counts with a baseline expression level of at least two RPM (reads per million of mapped reads) in at least three samples were TMM-normalized (edgeR package, (Robinson et al., 2009)) and log-transformed using voom function (Law et al., 2014). To identify differentially expressed sRNAs the empirical Bayes approach was used and the resultant p-values were adjusted using Benjamini and Hochberg's (FDR) method. Adjusted p-values below 0.05 were considered statistically significant.

Stem-loop RT-qPCR

Stem-loop RT-qPCR was used to quantify the expression of six target miRNAs in relation to the endogenous control (stu-mir167a-5p.1), which was determined to be the most robustly expressed in a sRNA sequencing dataset of potato plants that were uninfected or infected with a range of viruses (PVY, PLRV, PVS, PVX, PVT) (SRA accession no. SRP083247). TaqMan MicroRNA Assays (Thermo Fisher Scientific) were ordered according to the sRNA-Seq sequence of the selected miRNAs (**Supplemental Table 2**). Total RNA (1 µg) of the same samples as used for sRNA-Seq was DNase I (Qiagen) treated and reverse transcribed using SuperScript III First-Strand Synthesis System (Thermo Fisher Scientific) and stem-loop Megaplex primer pool (Thermo Fisher Scientific) following the manufacturer's protocol and previously optimized cycling parameters (Varkonyi-Gasic et al., 2007). No template control RT reactions were set to assess potential Megaplex primer pool background. qPCR reactions were performed in 10 µl volume on the LightCycler480 (Roche Diagnostics Ltd., Rotkreuz, Switzerland) in duplicates and two dilutions (8- and 80-fold) per sample using TaqMan Universal Master Mix II, no UNG (Thermo Fisher Scientific) and TaqMan MicroRNA Assays following the manufacturers' protocols. Additionally, for each miRNA assay, a standard curve was constructed from a serial dilution of the pool of all samples. Raw Cq values were calculated using the second derivative maximum method (Roche Diagnostics Ltd.) and miRNA expression was quantified using a relative standard curve method by normalization to the endogenous control (Baebler et al., 2011). The statistical significance was assessed by Student's t-test.

sRNA target prediction

In silico identification of potato transcripts targeted by identified sRNAs was carried out using the psRNATarget ((Dai and Zhao, 2011); http://plantgrn.noble.org/psRNATarget/) and StNIB_v1 sequences (Ramšak et al., 2014), following previously described parameters (Zhang et al., 2013). Moreover, targets of identified sRNAs were experimentally validated with parallel analysis of RNA ends (PARE) Degradome-Seq. The four degradome libraries (mock Désirée, PVY Désirée, mock NahG-Désirée, PVY NahG-Désirée) were constructed by pooling RNA of the biological replicates and sequenced on the Illumina HiSeq 2500 platform. The data were analyzed at LC Sciences (Houston, TX) with CleaveLand4 ((Addo-Quaye et al., 2009); http://sites.psu.edu/axtell/software/cleaveland4/) using all our experimentally identified sRNAs and the StNIB_v1 sequences allowing for maximum three mismatches. All identified degradation targets were classified into 5 categories as previously described (Addo-Quaye et al., 2009). Only categories 0-3 with high cleavage signal were considered as reliable cleavage. Results of miRNA-target (*PHAS* loci) interactions were also used to reveal miRNA triggers of the phasiRNA production. Only 22-nt miRNAs were kept as potential triggers (Chen et al., 2010; Cuperus et al., 2010).

Regulatory network construction

In order to compare the expression of sRNAs with the expression of their target transcripts we used a microarray gene expression dataset generated from the same samples ((Stare et al., 2015); GEO accession no. GSE58593). All differentially expressed miRNAs and phasiRNAs were analyzed for functional overrepresentation in biological pathways with MapMan software (Usadel et al., 2009) using the ontology adapted for potato (Rotter et al., 2007; Ramšak et al., 2014). All sRNAs and their targets, obtained by *in silico* prediction and Degradome-Seq were integrated with their expression data and used for construction of regulatory networks in Cytoscape 3.4 (Shannon et al., 2003).

Identification of *cis*-regulatory elements in promoter regions of *MIR* genes

1000 nt sequences upstream of the predicted *MIR* gene hairpin sequences were extracted as putative miRNA promoter regions (Megraw and Hatzigeorgiou, 2010) and scanned for *cis*-regulatory elements of plant transcription factors using position weight matrices and transcription binding sites in TRANSFAC (Matys et al., 2003); http://www.biobase-

international.com/product/transcription-factor-binding-sites) and PlantCARE (Lescot et al., 2002); http://bioinformatics.psb.ugent.be/webtools/plantcare/html/) databases.

Hormonal measurements

Hormone contents were determined by gas chromatography coupled with mass spectrometry (GC-MS). Approximately 100 mg of plant material was collected for each sample and 1 ml of 100% methanol (HPLC grade) was added. The following stable isotope-labeled compounds were added as internal standards to each sample prior to the extraction: 50 pmol [$^2H_4$]-SA, 50 pmol [$^2H_5$]-JA, 50 pmol [$^2H_2$]-IAA, 50 pmol [$^2H_2$]-GA A_3, 33 pmol [$^2H_6$]-ABA, 15 pmol [$^2H_5$]-OPDA. Next, the samples were heated at 60 °C for 5 min and then incubated at room temperature for 1 h with occasional vortexing. The methanolic phase was taken to complete dryness *in vacuo*. The resulting residue was dissolved in methanol (50 µl) to which diethyl ether (200 µl) was added. The samples were sonified (5 min) and centrifuged (5 min, 14,000 *g*). The particle-free supernatant was loaded to aminopropyl solid-phase extraction cartridges (Chromabond NH_2 shorty 10 mg; Macherey–Nagel GmbH, Düren, Germany). Each cartridge was washed twice with $CHCl_3$:2-propanol (2:1, v/v, 250 µl) before the hormone containing fraction was eluted with acidified diethyl ether (2 % acetic acid, v/v, 400 µl). The eluates were transferred into 0.8 ml autosampler vials and again taken to dryness in a gentle stream of nitrogen. Prior to MS assessment, the samples were derivatized with a 20 µl of a mix of acetone:methanol (9:1, v/v, 220 µl), diethyl ether (27 µl) and (trimethylsilyl)diazomethane solution (2.0 M in diethyl ether, 3 µl) and letting them rest for 30 min at room temperature. The setting for the GC and the MS were as described previously (Sanz et al., 2014). For the determination of endogenous and stable isotope-labeled methylated acidic plant hormones, respectively, the following ion transitions were recorded: MeSA m/z 152 to m/z 120 and m/z 156 to m/z 124 for [$^2H_4$]-MeSA, retention time 6.75 ± 0.4 min; MeOPDA m/z 238 to m/z 163 and m/z 243 to m/z 168 for [$^2H_5$]-MeOPDA, retention time 10.00 ± 0.4 min; MeJA m/z 224 to m/z 151 and m/z 229 to m/z 154 for [$^2H_5$]-MeJA, retention time 11.27 ± 0.5 min; MeIAA m/z 189 to m/z 130 and m/z 191 to m/z 132 for [$^2H_2$]-MeIAA, retention time 13.34 ± 0.4 min; MeABA m/z 162 to m/z 133 and m/z 168 to m/z 139 for [$^2H_6$]-MeABA, retention time 15.78 ± 0.4 min; and MeGA m/z 136 to m/z 120 and m/z 138 to m/z 122 for [$^2H_2$]-MeGA, retention time 21.67 ± 0.6 min. The amounts of endogenous hormone contents were calculated from the signal ratio of the unlabeled over the stable isotope-containing mass fragment observed in the parallel measurements. Significant changes in hormone concentrations between treatment-genotype groups were determined by ANOVA followed by

LSD post hoc analysis (Benjamini Hochberg FDR p-value adjustment, alpha= 0.05) using the Agricolae R package.

Gene set enrichment analysis

To identify SA regulated genes in cv. Désirée the normalized expression values between mock NahG-Désirée vs. Désirée and PVY-infected NahG-Désirée vs. Désirée samples were compared (calculated from the 3 dpi samples; data of Stare et al. (Stare et al., 2015). Gene Set Enrichment Analysis (GSEA; (Subramanian et al., 2005) was performed (false discovery rate corrected q $\leq$0.01) comparing expression profiles between both genotypes, using MapMan ontology as the source of the gene sets.

Data deposition and Gene IDs

The sRNA and Degradome-Seq data can be accessed at the NCBI's Gene expression omnibus (GEO) under accession numbers GSE84851 and GSE84967. Full list of gene/protein names used in this manuscript, together with their Gene IDs, short names, Arabidopsis orthologue genes is given in **S1 Table**.

Author Contributions

Conceptualization, M.K., M.P., D.D., Š.B., J.K., J.Z., and K.G.; Methodology, M.K., M.P., D.D., Ž.R., Š.B., S.P., K.G.; Formal Analysis, M.K., M.P., Ž.R., K.G.; Investigation, M.K., M.P., Š.B., S.P. and K.G.; Writing – Original Draft, M.K., K.G.; Writing – Review & Editing, M.K., M.P., D.D., Ž.R., Š.B., S.P., J.K., J.Z., and K.G; Visualization, M.K., M.P., K.G.; Supervision, K.G., Funding Acquisition, J.Z., K.G.

Funding

This research was funded by the Slovenian Research Agency (projects 1000-15-0105, J1-4268, P4-0165, N4-0026, J4-7636).

Acknowledgments

The authors would like to acknowledge dr. Tjaša Stare for providing plant material, dr. Sabine Rosahl for providing NahG-Désirée potato plants. Katja Stare and Tjaša Lukan for technical support, Maja Zagorščak for providing the script to determine the location of *MIR* loci in the potato genome, dr. Denis Kutnjak for the help with PVY^{NTN} genome assembly and dr. John Carr and dr. Anna Coll Rius for critical reading of the manuscript and fruitful discussions.

References

Addo-Quaye, C., Miller, W. and Axtell, M.J. (2009). CleaveLand: A pipeline for using degradome data to find cleaved small RNA targets. Bioinformatics. **25**:130–131.

Allen, R.S., Li, J., Stahle, M.I., Dubroué, A., Gubler, F. and Millar, A.A. (2007). Genetic analysis reveals functional redundancy and the major target genes of the Arabidopsis miR159 family. Proc. Natl. Acad. Sci. **104**:16371–16376. http://www.pnas.org/content/104/41/16371%5Cnhttp://www.ncbi.nlm.nih.gov/pubmed/17916625%5Cnhttp://www.pnas.org/content/104/41/16371.full.pdf%5Cnhttp://www.pnas.org/content/104/41/16371.short.

An, J., Lai, J., Sajjanhar, A., Lehman, M. and Nelson, C. (2014). miRPlant: an integrated tool for identification of plant miRNA from RNA sequencing data. BMC Bioinformatics. **15**:275. http://dx.doi.org/10.1186/1471-2105-15-275.

Antolin-Llovera, M., Petutsching, E.K., Katharina, M. and Parniske, M. (2014). Knowing your friends and foes – plant receptor-like kinases as initiators of symbiosis or defence. **2**:791–802.

Axtell, M.J., Jan, C., Rajagopalan, R. and Bartel, D.P. (2006). A Two-Hit Trigger for siRNA Biogenesis in Plants. Cell. **127**:565–577.

Baebler, Š. et al. (2011). Dynamics of responses in compatible potato - potato virus y interaction are modulated by salicylic acid. PLoS One. **6**: e29009.

Baulcombe, D. (2004). RNA silencing in plants. Nature. **431**:356–363.

Borges, F. and Martienssen, R.A. (2015). The expanding world of small RNAs in plants. Nat. Publ. Gr. **16**:1–15.

http://dx.doi.org/10.1038/nrm4085%5Cnpapers3://publication/doi/10.1038/nrm4085.

Bosch, F.V.A.N.D.E.N., Akudibilah, G., Seal, S.U.E. and Jeger, M. (2006). Host resistance and the evolutionary response of plant. 506–516.

Calvo, A.P., Nicolás, C., Nicolás, G. and Rodríguez, D. (2004). Evidence of a cross-talk regulation of a GA 20-oxidase (FsGA20ox1) by gibberellins and ethylene during the breaking of dormancy in Fagus sylvatica seeds. Physiol. Plant. **120**:623–630.

Carr, J.P., Lewsey, M.G. and Palukaitis, P. (2010). Signaling in Induced Resistance. In *Advances in Virus Research*. Elsevier Inc., pp. 57–121. http://dx.doi.org/10.1016/S0065-3527(10)76003-6.

Chan, P.P. and Lowe, T.M. (2016). GtRNAdb 2.0: an expanded database of transfer RNA genes identified in complete and draft genomes. Nucleic Acids Res. **44**:D184-9. http://nar.oxfordjournals.org/cgi/content/long/gkv1309v1.

Chellappan, P., Xia, J., Zhou, X., Gao, S., Zhang, X., Coutino, G., Vazquez, F., Zhang, W. and Jin, H. (2010). siRNAs from miRNA sites mediate DNA methylation of target genes. Nucleic Acids Res. **38**:6883–6894.

Chen, D., Meng, Y. and Yuan, C. (2011). Plant siRNAs from introns mediate DNA methylation of host genes Plant siRNAs from introns mediate DNA methylation of host genes. 1012–1024.

Chen, H.-M., Chen, L.-T., Patel, K., Li, Y.-H., Baulcombe, D.C. and Wu, S.-H. (2010). 22-Nucleotide RNAs trigger secondary siRNA biogenesis in plants. Proc. Natl. Acad. Sci. U. S. A.

Chen, H., Li, Y. and Wu, S. (2007). Bioinformatic prediction and experimental validation of a microRNA-directed tandem trans-acting siRNA cascade in Arabidopsis.

Coll, N.S., Epple, P. and Dangl, J.L. (2011). Programmed cell death in the plant immune system. Cell Death Differ. **18**:1247–1256. http://dx.doi.org/10.1038/cdd.2011.37.

Csorba, T., Kontra, L. and Burgyán, J. (2015). Viral silencing suppressors: Tools forged to fine-tune host-pathogen coexistence. Virology. **479–480**:85–103.

Cuperus, J.T. et al. (2010). Unique functionality of 22-nt miRNAs in triggering RDR6-dependent siRNA biogenesis from target transcripts in Arabidopsis. Nat. Struct. Mol.

730 Biol. **17**:997–1003. http://www.nature.com/doifinder/10.1038/nsmb.1866.

731 Curaba, J., Singh, M.B. and Bhalla, P.L. (2014). MiRNAs in the crosstalk between
732 phytohormone signalling pathways. J. Exp. Bot. **65**:1425–1438.

733 Dai, X. and Zhao, P.X. (2011). PsRNATarget: A plant small RNA target analysis server.
734 Nucleic Acids Res. **39**:1–5.

735 Devers, E.A., Branscheid, A., May, P. and Krajinski, F. (2011). Stars and Symbiosis :
736 MicroRNA- and MicroRNA * -Mediated Transcript Cleavage Involved in Arbuscular
737 Mycorrhizal Symbiosis 1 [W][OA]. **156**:1990–2010.

738 Du, Z., Chen, A., Chen, W., Westwood, J.H., Baulcombe, D.C. and Carr, J.P. (2014). Using a
739 viral vector to reveal the role of microRNA159 in disease symptom induction by a severe
740 strain of Cucumber mosaic virus. Plant Physiol. **164**:1378–88.
741 http://www.pubmedcentral.nih.gov/articlerender.fcgi?artid=3938627&tool=pmcentrez&r
742 endertype=abstract.

743 Floss, D.S., Levy, J.G., Lévesque-tremblay, V., Pumplin, N. and Harrison, M.J. (2013).
744 DELLA proteins regulate arbuscule formation in arbuscular mycorrhizal symbiosis.
745 **2013**:5025–5034.

746 Fonouni-Farde, C., Tan, S., Baudin, M., Brault, M., Wen, J., Mysore, K.S., Niebel, A.,
747 Frugier, F. and Diet, A. (2016). DELLA-mediated gibberellin signalling regulates Nod
748 factor signalling and rhizobial infection. Nat. Commun. **7**:12636.
749 http://www.nature.com/doifinder/10.1038/ncomms12636.

750 Ghachtouli, N.E., Martin-Tanguy, J., Paynot, M. and Gianinazzi, S. (1996). First report of the
751 inhibition of arbuscular mycorrhizal infection of Pisum sativum by specific and
752 irreversible inhibition of polyamine biosynthesis or by gibberellic acid treatment. **385**:.

753 Griffiths-Jones, S., Grocock, R.J., Dongen, S. van, Bateman, A. and Enright, A.J. (2006).
754 miRBase: microRNA sequences, targets and gene nomenclature. Nucleic Acids Res.
755 **34**:D140–D144.

756 Halim, V.A., Hunger, A., Macioszek, V., Landgraf, P., Nürnberger, T., Scheel, D. and Rosahl,
757 S. (2004). The oligopeptide elicitor Pep-13 induces salicylic acid-dependent and -
758 independent defense reactions in potato. Physiol. Mol. Plant Pathol. **64**:311–318.

759 Hohmann, U., Lau, K. and Hothorn, M. (2017). The Structural Basis of Ligand Perception

760 and Signal Activation by Receptor Kinases.

761 Huang, Y., Niu, B., Gao, Y., Fu, L. and Li, W. (2010). CD-HIT Suite: A web server for
762 clustering and comparing biological sequences. Bioinformatics. **26**:680–682.

763 Huot, B., Yao, J., Montgomery, B.L. and He, S.Y. (2014). Growth-defense tradeoffs in plants:
764 A balancing act to optimize fitness. Mol. Plant. **7**:1267–1287.

765 Ivanov, K.I., Eskelin, K., Bašic, M., De, S., Lõhmus, A., Varjosalo, M. and Mäkinen, K.
766 (2016). Molecular insights into the function of the viral RNA silencing suppressor
767 HCPro. Plant J. **85**:30–45.

768 Jin, Y. et al. (2016). DELLA proteins are common components of symbiotic rhizobial and
769 mycorrhizal signalling pathways. Nat. Commun. **7**:12433.
770 http://www.nature.com/doifinder/10.1038/ncomms12433.

771 Jones, J.D.G. and Dangl, J.L. (2006). The plant immune system. Nature. **444**:323–329.

772 Kamitani, M., Nagano, A.J., Honjo, M.N. and Kudoh, H. (2016). RNA-Seq reveals virus-
773 virus and virus-plant interactions in nature. FEMS Microbiol. Ecol. **92**:1–11.

774 Karasev, A. V and Gray, S.M. (2013). Continuous and emerging challenges of Potato virus Y
775 in potato. Annu. Rev. Phytopathol. **51**:571–86.
776 http://www.ncbi.nlm.nih.gov/pubmed/23915135.

777 Karasov, T.L., Chae, E., Herman, J.J. and Bergelson, J. (2017). Mechanisms to Mitigate the
778 Tradeoff between Growth and Defense.

779 Katagiri, F. (2003). Attacking Complex Problems with the Power of Systems Biology. Plant
780 Physiol. **132**:417–419.

781 Kozomara, A. and Griffiths-jones, S. (2014). miRBase : annotating high confidence
782 microRNAs using deep sequencing data. **42**:68–73.

783 Kutnjak, D., Rupar, M., Gutierrez-Aguirre, I., Curk, T., Kreuze, J.F. and Ravnikar, M. (2015).
784 Deep sequencing of virus derived small interfering RNAs and RNA from viral particles
785 shows highly similar mutational landscape of a plant virus population. J. Virol. **89**:4760–
786 9. http://jvi.asm.org/content/89/9/4760.abstract.

787 Law, C.W., Chen, Y., Shi, W. and Smyth, G.K. (2014). voom: Precision weights unlock
788 linear model analysis tools for RNA-seq read counts. Genome Biol. **15**:R29.

http://genomebiology.com/2014/15/2/R29.

Lelandais-Brière, C., Naya, L., Sallet, E., Calenge, F., Frugier, F., Hartmann, C., Gouzy, J. and Crespi, M. (2009). Genome-wide Medicago truncatula small RNA analysis revealed novel microRNAs and isoforms differentially regulated in roots and nodules. Plant Cell. **21**:2780–96. http://www.plantcell.org/content/21/9/2780.short.

Lescot, M., Déhais, P., Thijs, G., Marchal, K., Moreau, Y., Peer, Y. Van de, Rouzé, P. and Rombauts, S. (2002). PlantCARE, a database of plant cis-acting regulatory elements and a portal to tools for in silico analysis of promoter sequences. Nucleic Acids Res. **30**:325–7. http://www.pubmedcentral.nih.gov/articlerender.fcgi?artid=99092&tool=pmcentrez&rendertype=abstract.

Li, F., Pignatta, D., Bendix, C., Brunkard, J.O., Cohn, M.M., Tung, J. and Sun, H. (2011). MicroRNA regulation of plant innate immune receptors. Proc. Natl. Acad. Sci. U. S. A. **109**:1790–1795.

Li, H., Deng, Y., Wu, T.L., Subramanian, S. and Yu, O. (2010). Misexpression of miR482, miR1512, and miR1515 increases soybean nodulation. Plant Physiol. **153**:1759–1770.

Li, J., Brader, G. and Palva, E.T. (2004). The WRKY70 Transcription Factor: A Node of Convergence for Jasmonate-Mediated and Salicylate-Mediated Signals in Plant Defense. Plant Cell. **16**:319–331. http://www.plantcell.org/content/16/2/319%5Cnhttp://www.ncbi.nlm.nih.gov/pubmed/14742872%5Cnhttp://www.plantcell.org/content/16/2/319.full%5Cnhttp://www.plantcell.org/content/16/2/319.full.pdf.

Luis, A. De, Markmann, K., Cognat, V., Holt, D.B., Charpentier, M., Parniske, M., Stougaard, J. and Voinnet, O. (2012). Two microRNAs linked to nodule infection and nitrogen-fixing ability in the legume Lotus japonicus. Plant Physiol. **160**:2137–2154. http://www.ncbi.nlm.nih.gov/pubmed/23071252%5Cnhttp://www.ncbi.nlm.nih.gov/pmc/articles/PMC3510137/pdf/2137.pdf.

Mao, G., Turner, M., Yu, O. and Subramanian, S. (2013). miR393 and miR164 influence indeterminate but not determinate nodule development. Plant Signal. Behav. **8**:doi: 10.4161/psb.26753. http://www.ncbi.nlm.nih.gov/pubmed/24494229.

Matys, V. et al. (2003). TRANSFAC®: Transcriptional regulation, from patterns to profiles.

820 Nucleic Acids Res. **31**:374–378.

821 Megraw, M. and Hatzigeorgiou, A.G. (2010). MicroRNA Promoter Analysis. In J. M.
822 Walker, ed. *Plant MicroRNAs*. pp. 149–161.
823 http://www.springerlink.com/index/10.1007/978-1-60327-005-2.

824 Meyers, B.C. et al. (2008). Criteria for annotation of plant MicroRNAs. Plant Cell. **20**:3186–
825 3190.

826 Millar, A.A. and Gubler, F. (2005). The Arabidopsis GAMYB-Like Genes , MYB33 and
827 MYB65 , Are MicroRNA-Regulated Genes That Redundantly Facilitate Anther
828 Development. Plant Cell. **17**:705–721.
829 http://www.pubmedcentral.nih.gov/articlerender.fcgi?artid=1069693&tool=pmcentrez&r
830 endertype=abstract.

831 Moxon, S., Schwach, F., Dalmay, T., MacLean, D., Studholme, D.J. and Moulton, V. (2008).
832 A toolkit for analysing large-scale plant small RNA datasets. Bioinformatics. **24**:2252–
833 2253.

834 Navarro, L., Dunoyer, P., Jay, F., Arnold, B., Dharmasiri, N., Estelle, M., Voinnet, O. and
835 Jones, J.D.G. (2005). Repressing Auxin Signaling. Science (80-.).

836 Nawrocki, E.P. et al. (2015). Rfam 12.0: Updates to the RNA families database. Nucleic
837 Acids Res. **43**:D130–D137.

838 Ouyang, S., Park, G., Atamian, H.S., Han, C.S., Stajich, J.E., Kaloshian, I. and Borkovich, K.
839 a. (2014). MicroRNAs Suppress NB Domain Genes in Tomato That Confer Resistance
840 to Fusarium oxysporum. PLoS Pathog. **10**:.

841 Palatnik, J.F. et al. (2007). Sequence and Expression Differences Underlie Functional
842 Specialization of Arabidopsis MicroRNAs miR159 and miR319. Dev. Cell. **13**:115–125.

843 Park, J.H. and Shin, C. (2015). The role of plant small RNAs in NB-LRR regulation. Brief.
844 Funct. Genomics.1–7. http://bfgp.oxfordjournals.org/cgi/doi/10.1093/bfgp/elv006.

845 Peláez, P. and Sanchez, F. (2013). Small RNAs in plant defense responses during viral and
846 bacterial interactions: similarities and differences. Front. Plant Sci. **4**:343.
847 http://www.pubmedcentral.nih.gov/articlerender.fcgi?artid=3763480&tool=pmcentrez&r
848 endertype=abstract.

Ramšak, Ž., Baebler, Š., Rotter, A., Korbar, M., Mozetič, I., Usadel, B. and Gruden, K. (2014). GoMapMan: Integration, consolidation and visualization of plant gene annotations within the MapMan ontology. Nucleic Acids Res. **42**:1167–1175.

Ravnikar, M. (2013). Physiology of the Potato – Potato Virus Y Interaction. 1–31.

Ritchie, M.E., Phipson, B., Wu, D., Hu, Y., Law, C.W., Shi, W. and Smyth, G.K. (2015). Limma powers differential expression analyses for RNA-sequencing and microarray studies. Nucleic Acids Res. **43**:e47.

Robinson, M.D., McCarthy, D.J. and Smyth, G.K. (2009). edgeR: A Bioconductor package for differential expression analysis of digital gene expression data. Bioinformatics. **26**:139–140.

Roossinck, M.J. (2015). Move Over, Bacteria! Viruses Make Their Mark as Mutualistic Microbial Symbionts. J. Virol. **89**:6532–6535. http://jvi.asm.org/lookup/doi/10.1128/JVI.02974-14.

Rotter, A., Usadel, B., Baebler, S., Stitt, M. and Gruden, K. (2007). Adaptation of the MapMan ontology to biotic stress responses: application in solanaceous species. Plant Methods. **3**:10. http://www.plantmethods.com/content/3/1/10.

Ruiz-Ferrer, V. and Voinnet, O. (2009). Roles of plant small RNAs in biotic stress responses. Annu. Rev. Plant Biol. **60**:485–510.

Sanz, L., Fernandez-Marcos, M., Modrego, A., Lewis, D.R., Muday, G.K., Pollmann, S., Duenas, M., Santos-Buelga, C. and Lorenzo, O. (2014). Nitric Oxide Plays a Role in Stem Cell Niche Homeostasis through Its Interaction with Auxin(1 W OPEN). Plant Physiol. **166**:1972-U1195.

Scholthof, K.B.G. et al. (2011). Top 10 plant viruses in molecular plant pathology. Mol. Plant Pathol. **12**:938–954.

Seo, J.-K., Wu, J., Lii, Y., Li, Y. and Jin, H. (2013). Contribution of small RNA pathway components in plant immunity. Mol. Plant. Microbe. Interact. **26**:617–25. http://www.pubmedcentral.nih.gov/articlerender.fcgi?artid=3752434&tool=pmcentrez&rendertype=abstract.

Shannon, P., Markiel, A., Ozier, O., Baliga, N.S., Wang, J.T., Ramage, D., Amin, N., Schwikowski, B. and Ideker, T. (2003). Cytoscape: A software Environment for

integrated models of biomolecular interaction networks. Genome Res. **13**:2498–2504.

Shivaprasad, P. V., Chen, H.-M., Patel, K., Bond, D.M., Santos, B. a. C.M. and Baulcombe, D.C. (2012). A MicroRNA Superfamily Regulates Nucleotide Binding Site-Leucine-Rich Repeats and Other mRNAs. Plant Cell. **24**:859–874.

Si-Ammour, a., Windels, D., Arn-Bouldoires, E., Kutter, C., Ailhas, J., Meins, F. and Vazquez, F. (2011). miR393 and Secondary siRNAs Regulate Expression of the TIR1/AFB2 Auxin Receptor Clade and Auxin-Related Development of Arabidopsis Leaves. Plant Physiol. **157**:683–691.

Singh, R.P., Valkonen, J.P.T., Gray, S.M., Boonham, N., Jones, R.A.C., Kerlan, C. and Schubert, J. (2008). Discussion paper: The naming of Potato virus Y strains infecting potato. Arch. Virol. **153**:1–13.

Solomon-Blackburn, R.M. and Barker, H. (2001). Breeding virus resistant potatoes (Solanum tuberosum): A review of traditional and molecular approaches. Heredity (Edinb). **86**:17–35.

Stare, T., Ramšak, Ž., Blejec, A., Stare, K., Turnšek, N., Weckwerth, W., Wienkoop, S., Vodnik, D. and Gruden, K. (2015). Bimodal dynamics of primary metabolism-related responses in tolerant potato-Potato virus Y interaction. BMC Genomics. **16**:716. http://www.biomedcentral.com/1471-2164/16/716.

Subramanian, A. et al. (2005). Gene set enrichment analysis: a knowledge-based approach for interpreting genome-wide expression profiles. Proc. Natl. Acad. Sci. U. S. A. **102**:15545–50.

Usadel, B., Poree, F., Nagel, A., Lohse, M., Czedik-Eysenberg, A. and Stitt, M. (2009). A guide to using MapMan to visualize and compare Omics data in plants: A case study in the crop species, Maize. Plant, Cell Environ. **32**:1211–1229.

Varkonyi-Gasic, E., Wu, R., Wood, M., Walton, E.F. and Hellens, R.P. (2007). Protocol: a highly sensitive RT-PCR method for detection and quantification of microRNAs. Plant Methods. **3**:12.

Wang, D., Pajerowska-Mukhtar, K., Culler, A.H. and Dong, X. (2007). Salicylic Acid Inhibits Pathogen Growth in Plants through Repression of the Auxin Signaling Pathway. Curr. Biol. **17**:1784–1790.

909 Weiberg, A. and Jin, H. (2015). Small RNAs—the secret agents in the plant–pathogen
910 interactions. Curr. Opin. Plant Biol. **26**:87–94.
911 http://linkinghub.elsevier.com/retrieve/pii/S1369526615000862.

912 Westerhoff, H. V., Nakayama, S., Mondeel, T.D.G.A. and Barberis, M. (2015). Systems
913 Pharmacology: An opinion on how to turn the impossible into grand challenges. Drug
914 Discov. Today Technol. **15**:23–31.

915 Wilson, C. (2014). Management of Virus Disease: Host Resistance R. Cutts, ed., Wallingford,
916 Oxfordshire, UK CABI.

917 Wu, L., Zhou, H., Zhang, Q., Zhang, J., Ni, F., Liu, C. and Qi, Y. (2010). DNA Methylation
918 Mediated by a MicroRNA Pathway. Mol. Cell. **38**:465–475.
919 http://dx.doi.org/10.1016/j.molcel.2010.03.008.

920 Xu, X. et al. (2011). Genome sequence and analysis of the tuber crop potato. Nature.
921 **475**:189–195.

922 Yamaguchi, S. (2008). Gibberellin Metabolism and its Regulation. Annu. Rev. Plant Biol.
923 **59**:225–251.
924 http://www.annualreviews.org/doi/10.1146/annurev.arplant.59.032607.092804.

925 Yan, Z. et al. (2015). Identification of microRNAs and their mRNA targets during soybean
926 nodule development: Functional analysis of the role of miR393j-3p in soybean
927 nodulation. New Phytol. **207**:748–759.

928 Yang, D.L., Li, Q., Deng, Y.W., Lou, Y.G., Wang, M.Y., Zhou, G.X., Zhang, Y.Y. and He,
929 Z.H. (2008). Altered disease development in the eui mutants and Eui overexpressors
930 indicates that gibberellins negatively regulate rice basal disease resistance. Mol. Plant.
931 **1**:528–537. http://dx.doi.org/10.1093/mp/ssn021.

932 Yang, L., Mu, X., Liu, C., Cai, J., Shi, K., Zhu, W. and Yang, Q. (2015). Overexpression of
933 potato miR482e enhanced plant sensitivity to Verticillium dahliae infection. J. Integr.
934 Plant Biol. **57**:1078–1088.

935 Yoshihama, M., Nakao, A. and Kenmochi, N. (2013). snOPY: a small nucleolar RNA
936 orthological gene database. BMC Res. Notes. **6**:426.
937 http://www.biomedcentral.com/1756-0500/6/426.

938 Yu, D., Fan, B., MacFarlane, S. a and Chen, Z. (2003). Analysis of the involvement of an

inducible Arabidopsis RNA-dependent RNA polymerase in antiviral defense. Mol. Plant. Microbe. Interact. **16**:206–216.

Zhang, C., Li, G., Zhu, S., Zhang, S. and Fang, J. (2014). tasiRNAdb: a database of ta-siRNA regulatory pathways. Bioinformatics. **30**:1045–6. https://academic.oup.com/bioinformatics/article-lookup/doi/10.1093/bioinformatics/btt746%0Ahttp://www.ncbi.nlm.nih.gov/pubmed/24371150.

Zhang, R., Marshall, D., Bryan, G.J. and Hornyik, C. (2013). Identification and Characterization of miRNA Transcriptome in Potato by High-Throughput Sequencing. PLoS One. **8**:.

Zvereva, A.S. and Pooggin, M.M. (2012). Silencing and innate immunity in plant defense against viral and non-viral pathogens. Viruses. **4**:2578–2597.

Figure legends

Figure 1. **miR393-mediated cleavage of StTIR1 leads to production of phasiTIRs targeting diverse phytohormone signaling components**. Node shapes represent classes of sRNAs (triangle – miRNA; diamond – phasiRNA) or transcripts (circle). Node colors indicate components related to different hormone signaling pathways: green – jasmonic acid (JA); blue – auxin (AUX); magenta – brassinosteroid (BR); red – ethylene (ET). Arrows connect sRNAs and targets (blunt-end arrow) or *PHAS* loci and producing phasiRNAs (regular arrow). Node stu-miR393 represents miR393-5p and miR393-5p.1 and node StAFB1 represents StAFB1.1, StAFB1.2, and StAFB1.3. For details of the target transcripts/genes see **Supplemental Table 1**. StTIR1 – Transport inhibitor response 1, StLOX1 – Lipoxygenase 1, StERF2a – Ethylene responsive transcription factor 2a, StSAUR45 – Small auxin upregulated RNA 45, StAP2 – APETALA2, StOPR1 – 12-oxophytodienoate (OPDA) reductase, StDWF4 – Dwarf4, StARF1 – Auxin response factor 1, StEIN4 – Ethylene insensitive 4, StACD1 – 1-aminocyclopropane-1-carboxylic acid deaminase 1, StAFB1/2/3/5 – Auxin F-box 1/2/3/5.

Figure 2. **PVY induced changes in sRNA regulatory network are controlling multiple immune and gibberellin signaling components in Désirée at the onset of viral multiplication.** (**A**) Visualization of differentially expressed miRNAs/phasiRNAs in PVY^{NTN}-infected Désirée according to the function of their targets. Each square represents $\log_2$ ratios of expression between PVY^{NTN}- and mock-inoculated plants (red – upregulated; blue – downregulated). MapMan ontology bins: respiratory burst (20.1.1), redox state (21.6), MAPK (30.6), SA (17.8), JA (17.7), AUX (17.2), GA (17.6), BR (17.3), ET (17.5), CK (17.4), ABA (17.1), WRKY (27.3.32), NAC (27.3.27), GRAS (27.3.21), MYB (27.3.25), AP2/ERF (27.3.3), bHLH (27.3.6), PR-proteins (20.1.7), secondary metabolites (16), cell wall (10). The NBS-LRR and LRR-RLK bins were custom constructed for this study, based on their harboring domains (obtained from PFAM database; (Finn et al., 2016)). These bins represent differentially expressed miRNAs/phasiRNAs targeting NBS-LRRs or LRR-RLKs. NBS-LRR – nucleotide binding site-leucine-rich repeat protein, LRR-RLK – leucine-rich repeat receptor-like kinase, MAPK – mitogen activated protein kinase, SA – salicylic acid, JA – jasmonic acid, AUX – auxin, GA – gibberellin, BR – brassinosteroid, ET – ethylene, CK – cytokinin, ABA – abscisic acid,

PR – pathogenesis-related. (**B**) Network of differentially expressed endogenous sRNAs and vsiRNAs targeting mRNAs of GA biosynthesis and signaling pathways in Désirée 3 days post PVY^{NTN} inoculation. Node shape represent classes of sRNAs (triangle – miRNA; diamond – phasiRNA; arrowhead – vsiRNA), transcripts (circle) or metabolites (rectangle). Statistical significances of expression differences (p-values) and direction of expression change are represented by the node colors (see the legend). Arrows indicate type of interaction (solid-line normal arrow – direct interaction; dashed-line normal arrow – indirect interaction; blunt-end solid arrow – cleavage observed by Degradome-Seq, blunt-end dashed-line arrow – *in silico* predicted cleavage (or translational repression as proposed by Rogers and Chen (Rogers and Chen, 2013), dashed-line oval arrow – *in silico* predicted translational repression). Node stu-miR319a represents stu-miR319a-3p, stu-miR319a-3p.2, stu-miR319a-3p.4 and stu-miR319b-3p. Node StGA20ox represents StGA20ox, StGA20ox1, StGA20ox3 and StGA20ox4. For details of the target transcripts/genes see **Supplemental Table 1**. Stu-miR167e – stu-miR167e-3p; stu-miR482f – miR482f-3p; stu-miR6022 – miR6022-3p; StGA1 – GA REQUIRING 1 (ent-copalyl diphosphate synthase); StGA20ox – GA20-oxidase; StGA3ox – GA3-oxidase; StGID1C – GA receptor - GA INSENSITIVE DWARF1C hydrolase; StSN1 – Snakin-1; StDELLA – DELLA protein; StLRR-RLK – leucine-rich repeat receptor-like protein kinase. (**C**) Changes in concentrations of a set of plants hormones in Désirée 3 days after PVY^{NTN} infection. sRNA-mediated repression of GA biosynthesis was confirmed by reduced GA_3 levels in PVY-infected Désirée plants**.** Colors present as log_2 ratios of mean concentrations between PVY^{NTN}- and mock-inoculated plants (n=4; red – increased, blue – decreased level). * - indicate statistically significant values (ANOVA; $p < 0.05$). SA – salicylic acid, JA – jasmonic acid, OPDA –12-oxophytodienoic acid, ABA – abscisic acid, IAA – indole-3-acetic acid.

Figure 3. Numbers of unique and common differentially expressed miRNAs and phasiRNAs 3 days post PVY^{NTN} inoculation in comparison of SA-deficient and nontransgenic Désirée plants. Venn diagrams show the number of differentially expressed (FDR corrected p-value < 0.05) (**A**) miRNAs and (**B**) phasiRNAs in mock- or PVY^{NTN}-inoculated potato leaves of cv. Désirée and NahG-Désirée. Upregulated miRNAs/phasiRNAs are shown in bold and downregulated in normal text. D – Désirée, NahG – NahG-Désirée, M – mock, P – PVY^{NTN}.

Figure 4. sRNA response is attenuated in susceptible SA depleted plants following PVY^{NTN} infection. (**A**) Visualization of differentially expressed miRNAs/phasiRNAs in PVY^{NTN}-infected NahG-Désirée according to the function of their targets. Each square represents log_2 ratios of expression between PVY^{NTN}- and mock-inoculated plants (red – upregulated; blue – downregulated). (**B**) Network of endogenous sRNAs and vsiRNAs targeting mRNAs of GA biosynthesis and signaling pathways in NahG-Désirée 3 days post PVY^{NTN} inoculation. (**C**) Concentrations of a set of plants hormones in NahG-Désirée 3 days after PVY^{NTN} infection. The levels of all analyzed hormones remained unchanged in NahG plants following PVY^{NTN} infection. Colors present as log_2 ratios of mean concentrations between PVY^{NTN}- and mock-inoculated plants (n=4; red – increased, blue – decreased level). * - indicate statistically significant values (ANOVA; $p < 0.05$). For abbreviations and other details of the scheme, see the caption of **Figure 2**.

Figure 5. **sRNA regulatory network is intertwined with immunity- and gibberellin-related signaling mediating trade-offs in development and defense.** Node color denotes component type/function (grey – virus-derived; yellow – RNA silencing; blue – immune response; green – plant development). Lines represent different types of interaction (solid line – protein level; dashed – transcriptional/post-transcriptional level). Normal arrow – activation, blunt-end arrow – inhibition, combination of normal arrow and blunt-end arrow – unknown mechanism of action. ? – inferred from experiments performed in other species. vRNA – viral RNA; vsiRNA – virus-derived siRNA; HcPro – helper component-proteinase; DCL – DICER-like protein; AGO1 – Argonaute 1; RdRp – RNA-dependent RNA polymerase; NBS-LRR – nucleotide binding site-leucine-rich repeat protein; LRR-RLK – leucine-rich repeat receptor-like kinase; Ca – calcium; MAPK – mitogen activated protein kinase; SA – salicylic acid; GAMYB – GA-induced MYB-like protein; GA – gibberellin; GA20ox – GA20-oxidase; GA3ox – GA3-oxidase.

Table legends

Table 1. SA-dependent transcriptional responses of potato leaves in cv. Désirée.

Supplemental Online File legends

Supplemental Online File 1. sRNA regulatory network connecting endogenous miRNAs with phasiRNAs and their targets. For each predicted interaction, miRNA/phasiRNA identifiers, the target transcript identifiers, short gene name, full descriptions and MapMan ontology annotations (GoMapMan; (Ramšak et al., 2014)) are shown. Additionally, *PHAS* loci and their producing phasiRNAs are also included. Short names for potato genes were inferred from *Arabidopsis thaliana* orthologs where applicable, else the StNIB_v1 gene identifier was set (Ramšak et al., 2014). For each sRNA-target interaction, interaction properties were also included (see **Supplemental Dataset 5 and 6)**. Additionally, for each sRNA the log_2FC and p-values among different comparisons are given and the log_2FC ratios of target transcripts between PVY^{NTN} and mock inoculated Désirée or NahG-Désirée plants (from the study of Stare et al. 2015). – statistically not significant (FDR $p > 0.05$); NA – not analyzed or not available; NR – not relevant. D – Désirée; NahG – NahG-Désirée; M – mock; P – PVY^{NTN}.

Supplemental Online File 2. sRNA regulatory network connecting miRNAs, phasiRNAs, PVY-derived siRNAs (vsiRNAs) and their targets. For each predicted interaction, miRNA/phasiRNA identifiers, the target transcript identifiers, short gene name, full descriptions and MapMan ontology annotations (GoMapMan; Ramšak et al., 2014) are shown. Additionally, *PHAS* loci and their producing phasiRNAs are also included. Short names for potato genes were inferred from *Arabidopsis thaliana* orthologs where applicable, else the StNIB_v1 gene identifier was set (Ramšak et al., 2014). For each sRNA-target interaction, interaction properties were also included (see **Supplemental Dataset 5, 6 and 8**). Additionally, for each sRNA the log_2FC and p-values among different comparisons are given and the log_2FC ratios of target transcripts between PVY^{NTN} and mock inoculated Désirée or NahG-Désirée plants (from the study of Stare et al. 2015). – statistically not significant ($p > 0.05$); NA – not analyzed or not available; NR – not relevant. D – Désirée; NahG – NahG-Désirée; M – mock; P – PVY^{NTN}.